Carbohydrate–carbohydrate interaction provides adhesion force and specificity for cellular recognition

Iwona Bucior,[1,2] Simon Scheuring,[3] Andreas Engel,[3] and Max M. Burger[1,2]

[1]Friedrich Miescher Institute, 4058 Basel, Switzerland
[2]Marine Biological Laboratories, Woods Hole, MA 02543
[3]M.E. Müller Institute for Microscopy, Biozentrum, University of Basel, 4056 Basel, Switzerland

The adhesion force and specificity in the first experimental evidence for cell–cell recognition in the animal kingdom were assigned to marine sponge cell surface proteoglycans. However, the question whether the specificity resided in a protein or carbohydrate moiety could not yet be resolved. Here, the strength and species specificity of cell–cell recognition could be assigned to a direct carbohydrate–carbohydrate interaction. Atomic force microscopy measurements revealed equally strong adhesion forces between glycan molecules (190–310 piconewtons) as between proteins in antibody–antigen interactions (244 piconewtons).

Quantitative measurements of adhesion forces between glycans from identical species versus glycans from different species confirmed the species specificity of the interaction. Glycan-coated beads aggregated according to their species of origin, i.e., the same way as live sponge cells did. Live cells also demonstrated species selective binding to glycans coated on surfaces. These findings confirm for the first time the existence of relatively strong and species-specific recognition between surface glycans, a process that may have significant implications in cellular recognition.

Introduction

One of the fundamental features of a living cell is a prompt and adequate behavior during formation, maintenance, and pathogenesis of tissues. Short-term adhesion events, e.g., leukocyte recruitment (Robinson et al., 1999), development of the nervous system (Stipp and Hemler, 2000), or microbial pathogenesis (Feizi and Loveless, 1996) require reversible, but still specific molecular surface interactions, rather than tight and stable adhesions between stationary cells (Spillmann and Burger, 1996). Carbohydrates, the most prominently exposed structures on the surface of living cells, with flexible chains and many potential binding sites are ideal to serve as important players in these events. Molecular interactions where carbohydrates are involved are usually considered as weak interactions (Varki, 1994; Spillmann and Burger, 1996), and therefore, biological relevance of carbohydrate–carbohydrate interactions is often questioned. Hakomori's group has been first to show glycosphingolipid self-interactions to occur by way of Lewis[x] determinant (Galβ1→4[Fucα1→3]

GlcNAcβ1→3Galβ1→4Glcβ) (Le[x]) to Le[x] carbohydrate-dependent cell adhesion in the compaction of mouse embryo (Eggens et al., 1989) and autoaggregation of human embryonal carcinoma cells (Song et al., 1998). Extended studies revealed specific cellular recognition between lymphoma and melanoma cells based on gangliotriaosylceramide (GalNAcβ1→4Galβ1→4Glcβ1→1Cer)–sialosyllactosylceramide (NeuAcα2→3Galβ1→4Glcβ1→1Cer) interaction, and sialosyllactosylceramide (NeuAcα2→3Galβ1→4Glcβ1→1Cer)-dependent adhesion of melanoma cells, which led to spreading and enhancement of cell motility (Kojima and Hakomori, 1989; Iwabuchi et al., 1998).

The very first experimental demonstration of cellular recognition and adhesion phenomena in the animal kingdom came from an invertebrate system, i.e., from marine sponges (Wilson, 1907), and was later assigned to cell surface proteoglycans (Humphreys, 1963). Dissociated sponge cells from two different species have the capacity to reaggregate through surface proteoglycans (Fernandez-Busquets and Burger, 2003) in a Ca^{2+}-rich environment (10 mM, i.e., physiologic for seawater) by sorting out according to their

Figure 1. Specific recognition between live cells, and between cells and glycan-coated beads. (A) Homotypic aggregation between *Microciona prolifera* red cells during a 4-h rotation-mediated aggregation in seawater with physiological Ca^{2+}. (B) Species specific sorting out between cells from two different sponge species with red (*Microciona prolifera*) and yellow (*Suberites fuscus*) natural pigment. (C) Inhibition of the cell–cell aggregation in the absence of Ca^{2+}. (D) Inhibition of the homotypic aggregation between *Microciona* cells by the antibody directed against the carbohydrate epitope of *Microciona* proteoglycan. (E) Homotypic aggregation between yellow cells (*Suberites*) and their own surface glycans coated on red beads during a 4-h rotation-mediated aggregation in seawater with physiological Ca^{2+}. (F) Species specific sorting out between yellow cells and red beads carrying glycans from cells from another sponge species. (G) Inhibition of the cell–glycan aggregation in the absence of Ca^{2+}. (H) Inhibition of the homotypic aggregation between red *Microciona* cells and their glycan coated on red beads by the antibody directed against the carbohydrate epitope of *Microciona* proteoglycan.

the same type   different types   no calcium   antibody
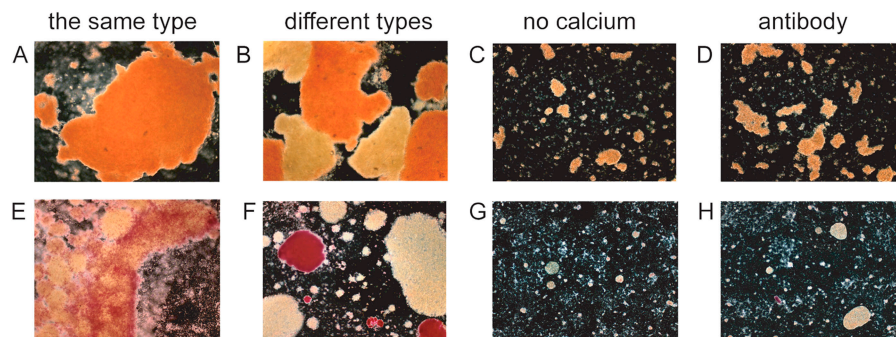
species of origin, in the same way as dissociated embryonic cells from two different vertebrate tissues sort out according to their tissue of origin. Consequently, this simple and highly specific cellular recognition phenomenon in sponges has been used for almost a century as a model system to study recognition and adhesion events in multicellular organisms. Sponge cell–cell aggregation involves Ca^{2+}-independent binding of proteoglycans to a cell surface and Ca^{2+}-dependent self-association of proteoglycans (Turner and Burger, 1973; Jumblatt et al., 1980). A monoclonal antibody raised against the purified proteoglycan from *Microciona prolifera* sponge inhibited the proteoglycan self-association and the epitopes were identified as short carbohydrate units of the 200-kD glycan (Misevic and Burger, 1993): a sulfated disaccharide (Spillmann et al., 1995) and a pyruvylated trisaccharide (Spillmann et al., 1993). Recently, Vliegenthart's group could demonstrate self-interactions of the sulfated disaccharide using surface plasmon resonance (Haseley et al., 2001). However, species-specific interactions between 200-kD glycans from different sponge species have not yet been demonstrated in order to prove the existence of species-specific carbohydrate–carbohydrate recognition system.

200-kD glycan moieties from adhesion proteoglycans from four different marine sponge species were purified here and the species specificity of a glycan–glycan interaction was investigated in aggregation and adhesion assays. Atomic force microscopy (AFM) measurements were performed to measure the binding strength between single interacting glycan molecules and to demonstrate quantitative differences in binding forces between different species of 200-kD glycans. Results confirm the concept of the relatively strong and species-specific carbohydrate–carbohydrate interaction as an important player in cellular recognition.

Results

### Live cells specifically aggregate with glycan-coated beads

In the classical assay for specific cell–cell recognition, live sponge cells can recognize their own kind and form big homogeneous aggregates on a shaker at the right shear forces, i.e., rotor speed, as shown for red cells of *Microciona prolifera* (Fig. 1 A). At too high rotation speed no cell aggregates are

formed because shear forces are too high. At too low rotation speed unspecific, faulty initial contacts will remain because such cells do not get a second or third chance to form higher affinity adhesions with other cells. When cells from two different sponge species were shaken together in suspension (red cells, *Microciona prolifera*; yellow cells, *Suberites fuscus*), they sorted out into separate aggregates consisting of cells from the same species only (Fig. 1 B), and no heterotypic mixtures consisting of cells from different species would form. Specific cellular recognition could be inhibited by the absence of Ca^{2+} ions (Fig. 1 C). Recognition between *Microciona* (red) cells could be inhibited by the antibody directed against the carbohydrate epitope of the *Microciona* proteoglycan (Fig. 1 D), and much smaller cell aggregates could be seen as compared with aggregation in physiological Ca^{2+} (Fig. 1 A). There was no visible effect of the antibody on homotypic interactions between cells from other species (unpublished data).

In a cell–glycan recognition assay, live cells were allowed to aggregate with glycan-coated red beads (1-μm diam) similar in size to small sponge cells (2-μm diam), under the same shear forces, i.e., rotor speed as for cell–cell aggregation. Yellow cells (*Suberites*) specifically recognized red beads coated with their own glycans and formed large mixed aggregates (Fig. 1 E). Yellow cells, however, did not mix but separated from aggregates of red beads coated with glycans from a different species, namely *Microciona* (Fig. 1 F). As in cell–cell recognition, the absence of Ca^{2+} ions (Fig. 1 G) inhibited the cell–glycan recognition. The antibody directed against the carbohydrate epitope of *Microciona* proteoglycan could only inhibit the homotypic interaction between red *Microciona* cells and their glycans coated on red beads (Fig. 1 H). Aggregation between cells from other species and their glycans coated on red beads could not be inhibited by that antibody (unpublished data).

Aggregation of glycan-coated beads mimics species-specific cellular aggregation

An assay for glycan–glycan recognition was designed, which mimics the classical assay for specific aggregation of sponge cells. Glycan-coated red and green beads the size of small sponge cells were allowed to aggregate under identical shear
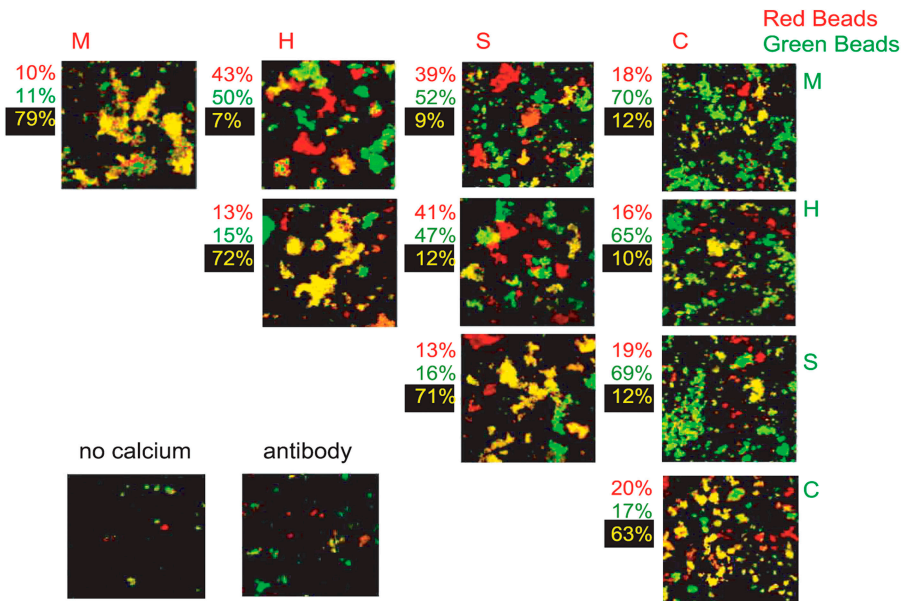
Figure 2. **Specific recognition between glycan-coated beads.** Red and green glycan-coated beads sorted out specifically during a 4-h rotation-mediated aggregation in seawater with physiological Ca^{2+}. Yellow areas depict clumps of mixed red and green beads coated with identical glycans. Red and green areas reflect clumps of separated beads coated with different glycans. The colored numbers on the left side of each picture represent the percentage of clumps of the respective color. The glycan–glycan recognition could be inhibited by the absence of Ca^{2+} ions. The antibody directed against the carbohydrate epitope of *Microciona* proteoglycan inhibited homotypic aggregation between *Microciona* glycans coated on red and green beads. M, *Microciona*; H, *Halichondria*; S, *Suberites*; C, *Cliona*.

forces, i.e., rotor speed as used for cell–cell recognition assays. Beads coated with glycans from identical proteoglycans formed 63–79% yellow aggregates, which are the result of intermingling of red and green beads (Fig. 2). In stark contrast, beads coated with glycans derived from proteoglycans from different species did separate into red and green aggregates. In this case yellow aggregates, i.e., heterotypic mixtures of glycans originating from different species, never formed >12% of aggregated patches.

There were two possible modes for the color distribution in the glycan-coated bead–bead aggregation: either it was random or species specific. Random distribution, which can be described by Pascal's triangle (Pickover, 2001), applies to the homotypic glycan-coated bead–bead aggregation, i.e., between glycans from the same species. In this case, red and green beads coated with identical glycans were mixing in a casual manner leading to a high number of yellow patches. However, based on Pascal's triangle analysis, the color distribution in the heterotypic glycan-coated bead–bead aggregation, i.e., between glycans from two different species, was not random but species specific. Red and green beads coated with glycans from two different species were specifically sorting out into separate red and green aggregates.

As in cell–cell and cell–glycan recognition, the absence of Ca^{2+} ions inhibited the glycan–glycan recognition. The antibody directed against the carbohydrate epitope of the *Microciona* proteoglycan inhibited the homotypic interaction between *Microciona* glycans coated on red and green beads. There was no visible effect of the antibody on homotypic interactions between other species glycans (unpublished data). Results obtained with glycan-coated beads (Fig. 2) reflect thus the same results obtained with live cells (Fig. 1, A–D).

It has been reported previously that 400 molecules of *Microciona* proteoglycan bound per cell cause live cells to aggregate (Jumblatt et al., 1980). The number of 200-kD glycan copies per proteoglycan molecule was determined from the mass of total carbohydrate recovered in 200-kD glycan fractions either after gel electrophoresis or gel filtration (Misevic

and Burger, 1993). Because 37% of the total carbohydrate content of the proteoglycan molecule occurred in the form of 200-kD glycan ($\sim$70% of the proteoglycan mass is carbohydrate; proteoglycan $M_r = 2 \times 10^7$), one proteoglycan carries $\sim$26 copies of this glycan. Therefore, $\sim$10,400 glycan molecules (400 proteoglycan molecules) per cell cause living cells to aggregate. In our experiments, binding measurements indicated that $\sim$2,500 molecules of 200-kD glycan per bead specifically aggregated glycan-coated beads. The number was calculated from the specific absorbance of stained glycans after reversing the binding to beads (which gave the number of moles: 0.192×10^{-11}) and Avogadro's number, and was divided by the number of beads (4.5×10^8). Surface areas of the cell and the bead were calculated from diameters, and they were 12.56 μm^2 and 3.14 μm^2 accordingly. This led to the final assessment that the glycan density per cell and per bead causing species-specific live cell and glycan-coated bead recognition and aggregation is similar: 828 molecules/μm^2 for cell–cell aggregation and 810 molecules/μm^2 for glycan-coated bead–bead aggregation.

Live cells and cell surface glycans adhere species specifically to glycans coated on a plastic surface

The binding of live cells to glycans from their surface proteoglycans coated onto a solid polystyrene phase was assessed (Fig. 3, A–D). The binding to glycans from proteoglycans from different species of origin was three to five times lower. Cell adhesion showed clear dependence on the quantity of the glycan coated, and could be abolished in the absence of Ca^{2+} ions. Pretreatment of *Microciona* cells with the antibody directed against the carbohydrate epitope of their surface proteoglycan inhibited 86% of these cells from adhesion to their own glycan (Fig. 3 E). In this assay, little cross-reactivity of the antibody (Misevic et al., 1987) could be detected because it blocked only 23% or less adhesion between other cells and their 200-kD glycans.

Similarly to cell–glycan adhesion, 200-kD glycans adhered strongly to surface-bound glycans from identical pro-
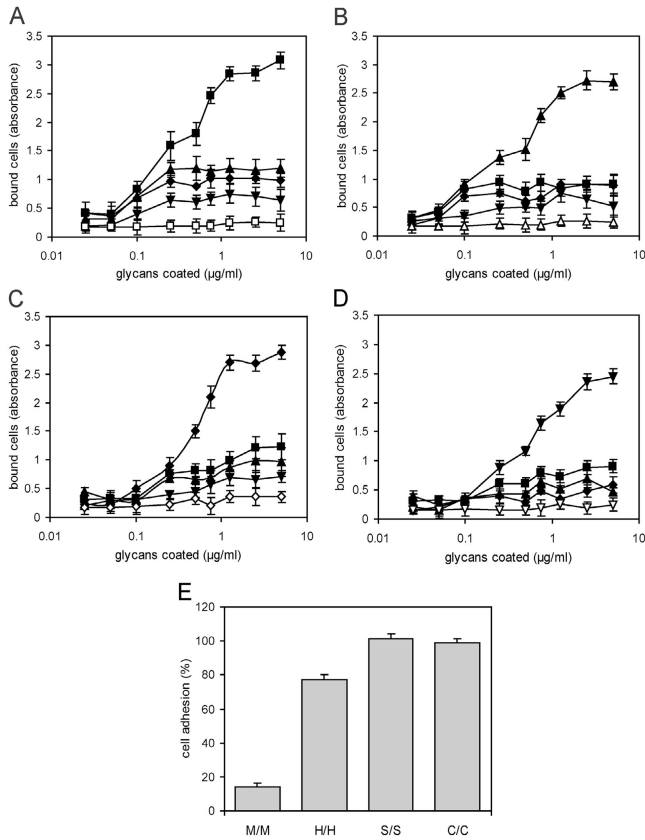
Figure 3. Adhesion of live cells to glycan-coated plates.
(A) *Microciona*, (B) *Halichondria*, (C) *Suberites*, and (D) *Cliona* live cells were incubated for 2 h in seawater with physiological Ca^{2+} in 96-well flat bottom polystyrene plastic plates coated with *Microciona* (■), *Halichondria* (▲), *Suberites* (◆), and *Cliona* (▼) glycans isolated from surface proteoglycans of mother sponges. (□, △, ◇, ▽) Binding of the respective cells to their glycans coated on plates without the presence of Ca^{2+}. (E) Effect of the carbohydrate directed *Microciona* proteoglycan antibody on cell adhesion to glycan-coated plates. Error bars represent SD of four to six independent experiments. M, *Microciona*; H, *Halichondria*; S, *Suberites*; C, *Cliona*.
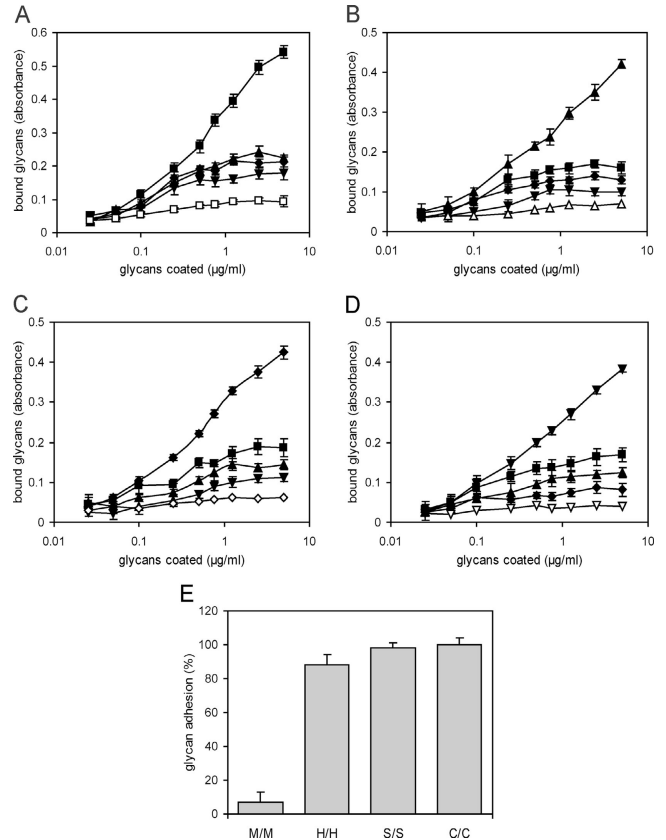
Figure 4. Adhesion of surface glycans to glycan-coated plates.
(A) *Microciona*, (B) *Halichondria*, (C) *Suberites*, and (D) *Cliona* glycans were incubated for 2 h in seawater with physiological Ca^{2+} in 96-well flat bottom polystyrene plastic plates coated with various quantities of *Microciona* (■), *Halichondria* (▲), *Suberites* (◆), and *Cliona* (▼) glycans isolated from surface proteoglycans. (□, △, ◇, ▽) Binding of the respective glycans to their glycan-coated plates in the absence of Ca^{2+}. (E) Effect of the carbohydrate directed *Microciona* proteoglycan antibody on glycan adhesion to glycan-coated plates. Error bars represent SD of four to six independent experiments. M, *Microciona*; H, *Halichondria*; S, *Suberites*; C, *Cliona*.

teoglycans in a dose-dependent manner (Fig. 4, A–D). The adhesion to glycans from different species was 2.5–6 times lower. This specific glycan–glycan adhesion could only be observed in the presence of Ca^{2+} ions. The antibody against the carbohydrate epitope of *Microciona* proteoglycan blocked 93% of the adhesion between its 200-kD glycans and produced little cross-reactivity (Misevic et al., 1987) by blocking 12% or less of the adhesion between glycans from other proteoglycans (Fig. 4 E).

The glycan–glycan adhesion force is in the piconewton range

Intermolecular adhesive force measurements between 200-kD glycan molecules coated on a probe tip and a surface (Fig. 5 A) were performed using AFM (Rief et al., 1997; Alonso and Goldmann, 2003). Based on fluorescence imaging with labeled glycans, no clustering of glycans was observed either on the probe tip or the surface. During retraction of the tip the glycan structure was lifted, stretched and finally noncovalent bonds between two molecules were be-

ing broken one by one. The existence of multiple noncovalent bonds between carbohydrates of glycan molecules is suggested by the presence of multiple peaks on the force curves, as recorded in the presence of Ca^{2+} (Fig. 5 B, lines 3–8). There was no interaction recorded between gold–gold (Fig. 5 B, line 1) or in the absence of Ca^{2+} (Fig. 5 B, line 2). Force measurements taken directly at the surface (<10 nm) were due to nonspecific interactions between the cantilever tip and the surface (Carrion-Vazquez et al., 2000), e.g., the first rupture peak in Fig. 5 B (lines 3, 5, and 8) and the first two in Fig. 5 B (lines 4 and 7). Only those measured at distances >10 nm from the surface were considered as direct interactions between glycan molecules. Strong multiple interactions were observed between glycans from the same species and noncovalent bonds between two interacting glycan molecules of the same origin (one peak) were ruptured at the forces between 190 and 310 piconewtons (pN; Fig. 6 A). The strength of the attachment of 200-kD glycans through S to the Au surface of the probe tip and the substrate is much stronger: 1.4 nanonewtons (Grandbois et al., 1999).
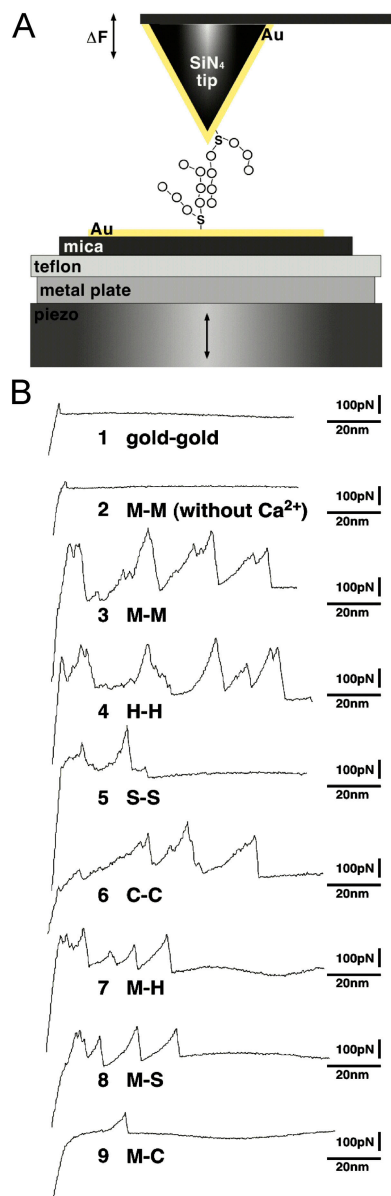
Figure 5.   AFM measurements of glycan–glycan binding forces.
(A) Scheme of AFM set up for the measurement of the intermolecular forces between glycan molecules in seawater with physiological Ca^{2+}. (B) Examples of AFM force curves. Lines 1 and 2 represent control curves: (1) gold–gold interaction and (2) glycan–glycan interaction in seawater without Ca^{2+}. Lines 3–6 represent curves of interactions between glycans from the same species in seawater with physiological Ca^{2+}, whereas lines 7–9 represent curves of interactions between different species of glycans. M, *Microciona*; H, *Halichondria*; S, *Suberites*; C, *Cliona*.

Table I. Trace amino acid composition of 200-kD glycans

	Microciona	*Halichondria*	*Suberites*	*Cliona*
	mol amino acid/mol glycan			
Asp	0.9	0.7	0.8	0.5
Glu	0.4	0	0	0
Ser	0	0.1	0.2	0
His	0	0	0	0
Gly	0.3	0.3	0.5	0.3
Thr	0.2	0.1	0	0
Ala	0.3	0.2	0.3	0.3
Arg	0	0	0	0
Tyr	0	0	0	0
Val	0	0	0	0
Met	0	0	0	0
Phe	0	0	0	0
Ile	0	0	0	0
Leu	0	0	0.1	0
Lys	0	0.1	0	0
Pro	0	0	0	0
Asn	0	0	0	0
Gln	0	0	0	0
Trp	0	0	0	0
Ca	0	0	0	0
Total	2.1	1.5	1.9	1.1

The values are the average from two determinations. Cys was ND.

calculated from Mann-Whitney test, were clearly below 0.01 and showed that the difference is statistically significant.

Specificity of the carbohydrate–carbohydrate interaction is also reflected in the polyvalence

The characteristic feature of the glycan–glycan interaction is the repetition of interactive sites along the glycan chain, which further increases the strength of the interaction and thus the specificity. The distance between the peak numbers 1 and 2 (2 and 3, etc.) on force curves was measured to produce a histogram of the peak periodicity (Fig. 6 B). 80% of force curves between glycans from the same species of cells showed more than one interaction peak, with a distance between binding motifs of ~20 nm. In contrast, <35% of force curves between glycans from different species of cells showed multiple interaction peaks, demonstrating the preference for one rather unspecific binding event during the interaction.

The glycan molecules used here have chain-like structures of an average folded length of ~40 nm as imaged by AFM (Jarchow et al., 2000), whereas the extended structure has a length of up to 180 nm (Dammer et al., 1995). 75% of the total lengths of the force curves for the same species glycans were 20–50 nm, and in some cases the curves showed extensions up to 130 nm (Fig. 6 C). This then indicates that the interaction sites are located along the carbohydrate chain and not only at its end. In contrast, 70% of the force curves for glycans from two different species showed total interaction lengths of 10–30 nm only.

Pronase digestion of glycans is essentially complete

Proteoglycan molecules were subjected to an extensive pronase digestion in order to obtain protein-free glycans.

Single glycan–glycan adhesion force is species specific

In stark contrast to strong binding forces between glycans from the same species, clearly reduced forces were recorded between glycans from different species (Fig. 6 A). The single noncovalent bond between two interacting glycan molecules from two different species was ruptured at the forces between 110 and 210 pN. In a statistical analysis, the binding forces between glycans from the same species were always stronger than those between glycans from different species. P values for the difference in binding force between the two,

Figure 6.   A quantitative evaluation of species specific versus nonspecific AFM measurements. (A) Adhesion force values of the interactions between glycans from the same species or from different species attached to the AFM tip and the mica surface. On the ordinate number of rupture events are provided normalized to 1.0 for the category of the highest number of events. (B) Periodicity measurements showing distances between rupture peaks, which indicate the distances between binding motifs on the carbohydrate chain. The white bar reflects the number of probe lift events where only one rupture event could be registered. (C) The length of the force curves measured from the lift-off point to the last peak, indicating the total length of the interacting carbohydrate chain. M, *Microciona* glycan; H, *Halichondria* glycan; S, *Suberites* glycan; C, *Cliona* glycan.
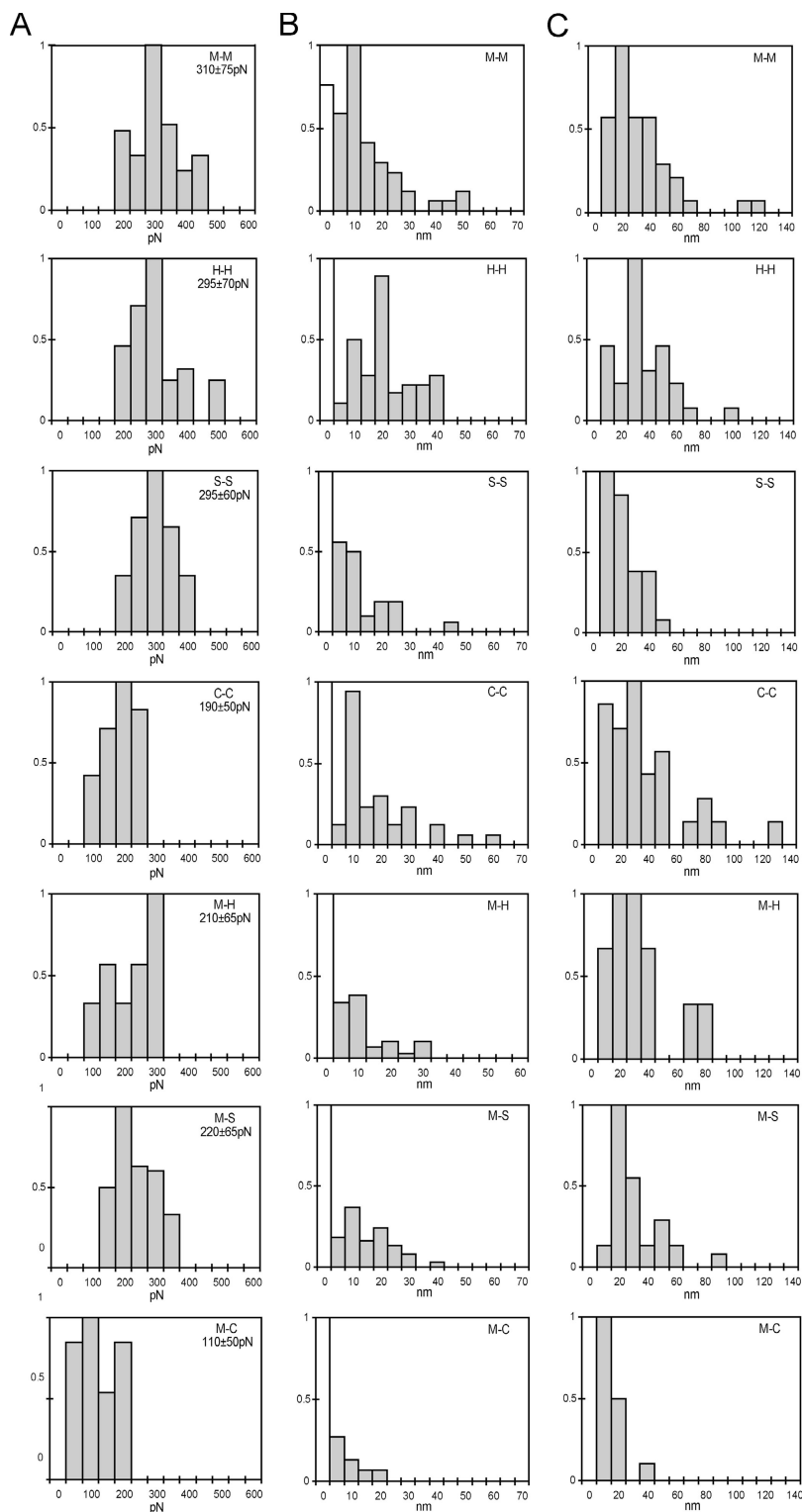
The total 200-kD glycans were separated from free amino acids and peptides by gel filtration and ion-exchange chromatography (Misevic et al., 1987). The 200-kD glycan has an apparent $M_r = 200 \times 10^3 \pm 40 \times 10^3$, and electrophoretic and chromatographic separation techniques indicated that the glycan is a single molecular species with possible charge and size microheterogeneities (Misevic et al., 1987). There have been essentially no

losses of carbohydrates during the purification procedures because the carbohydrate yield of the glycan fractions was ~97%. Amino acid analysis of glycans from the four sponge species used showed that there was from 0.5 (*Cliona celata*) to 0.9 (*Microciona prolifera*) mole of linker aspartate/mol of glycan (Table I). Only trace amounts of a few other amino acids were detected. This indicates that the digestion was complete and that the purification pro-

cedure for the 200-kD glycans led to essentially pure glycan fractions, free of any protein contaminations.

Discussion

Virtually all animal cells produce proteoglycans, which vary greatly in structure, expression, and functions (Kjellen and Lindahl, 1991). Nevertheless, they do have a general propensity to be ECM components and to mediate specific interactions related to different aspects of cell adhesion phenomena through their protein or carbohydrate portions (Truant et al., 2003). In contrast to the rapid progress in studies of cell recognition and adhesion through protein–protein or protein–carbohydrate interactions (Feizi, 2000; Hynes and Zhao, 2000), the number and progress of studies on the possible role of carbohydrate–carbohydrate interactions in these events is still very small. Cell recognition and adhesion processes controlling the remarkable ability of sponge cells to species specifically aggregate after mechanical dissociation to finally reconstitute a functional sponge with canals, mineral skeleton, and collagen fibrils and fibers (Wilson, 1907; Galtsoff, 1925) is mediated by proteoglycans and this function may reside in the glycan portion. Data presented here significantly broaden the current views on the role of carbohydrates in cellular recognition by a novel demonstration of the species-specific character of the glycan–glycan interaction based on relatively strong single binding forces in the range of several hundred pN, providing an adequate affinity and avidity to mediate specific cell–cell recognition.

The examination of carbohydrate–carbohydrate interactions at the atomic level is critical in understanding the nature of these interactions and their biological role. Measured adhesive forces between identical glycans (190–310 pN) compare well with the range of forces between the entire proteoglycan molecules, which vary from 50 to 400 pN, depending on the number of binding sites ruptured (Dammer et al., 1995; Popescu et al., 2003). Similar values are also reported for other biologically relevant forces, e.g., for single protein–glycan interactions (Fritz et al., 1998; Hanley et al., 2003), when interaction of P-selectin from leukocytes with its carbohydrate ligand from endothelial cells was measured (165 pN), or for single antibody–antigen recognition (Hinterdorfer et al., 1996; Saleh and Sohn, 2003) with rupture forces of 244 pN. The force spectra shown in Fig. 5 exhibit the general shape anticipated for simple entropic polymers that extend until the carbohydrate–carbohydrate interaction ruptures. Considering molecular compliance it should be noted that the rupture forces measured here are below those inducing the chair-boat transition, which could have interfered with the interpretation of the results.

The density of glycans on the AFM probe tip and the substrate was adjusted to meet the expectation that the surface layers are neither multilayered nor clustered, and therefore, direct glycan–glycan interactions were measured. The exact number of single rupture events between two interacting glycan molecules is difficult to define with certainty because it cannot be excluded that a so-called "single event" may be a composite of more than one bond rupture. Nevertheless, because the statistical analysis of pull-off distances show that the overall lengths of force curves (from 20 nm up to 130 nm) are less than the expected extended length of the glycan (160–180 nm), it can be assumed that single glycan molecule and not multiple glycan molecule interactions were measured here.

The specificity of glycan-mediated recognition is guaranteed both by the higher adhesion forces per binding site as well as by the higher amount of polyvalent interactions between glycans from the same species versus glycans from different species. The repetition of the binding motif along the carbohydrate chain ensures sufficient binding strength to function in vivo. Polyvalence can be controlled by various means: e.g., by surface density of presented structures, ionic strength modulating attractive versus repulsive forces, subtle changes in biosynthesis of the carbohydrate sequences, etc. These allow changing the affinity of the interactive molecules and therefore, creating a highly flexible and specific model of recognition system. The model assumes gradual adhesion during initial contact between two different cells or cell and matrix by allowing cells to test surrounding surfaces and first create weak random contacts before releasing or reinforcing adhesion (Burger, 1979). Therefore, interactions between two different species of glycans could still be recorded in AFM measurements, though of lower stability than these between glycans from the same species. Similarly, some amount of heterotypic aggregates consisting of different species of glycans was present in glycan-coated bead aggregation experiments.

Ca^{2+} ions or other divalent cations are crucial in carbohydrate–carbohydrate interactions. Here, the presence of Ca^{2+} ions was essential. No interaction between cells, cells and surface glycans, and between surface glycans could be observed in the absence of Ca^{2+}. Also no adhesion forces between single glycan molecules could be detected during AFM measurements. However, it has been reported that the presence of Ca^{2+} ions did not contribute significantly to the adhesion force in Le^x–Le^x interaction (Tromas et al., 2001). On the other hand, self-aggregation of Le^x molecules in aqueous solution, where the molecules move freely, occurred only in the presence of Ca^{2+} ions (de la Fuente et al., 2001). On the molecular level, Ca^{2+} ions probably provide coordinating forces (Haseley et al., 2001), though ionic forces cannot be excluded. These Ca^{2+} interactions are thought to stabilize conformations and can thereby lead to hydrogen bonds and hydrophobic interactions elsewhere in the glycan molecule (Spillmann and Burger, 1996). Further studies are required to resolve the exact role of Ca^{2+} and other divalent cations in carbohydrate–carbohydrate interactions.

Inhibition of sponge cell recognition and aggregation by species-specific carbohydrate epitope antibodies as shown earlier (Misevic et al., 1987; Misevic and Burger, 1993) do not prove glycan–glycan interactions to be relevant because they leave the option of glycan–protein interactions open. The same interpretation holds for two of the approaches presented here: species specificity for the glycan-coated bead interaction with live sponge cells (Fig. 1, E–H) and for the live cells binding to glycan-coated plastic surfaces (Fig. 3). The specificity found here for glycan–glycan interaction (Fig. 4), for glycan-coated bead sorting (Fig. 2), and the force and specificity shown in the AFM measurements (Fig. 6) make, however, a role for carbohydrate–carbohydrate in

sponge cell recognition and adhesion likely. The fact that the outermost cell surface is made up primarily of a dense layer of hydrophilic glycans supports the notion that upon first contact between cells such reversible and flexible glycan–glycan interactions may play a pivotal role in cell recognition processes.

Materials and methods

Sponges, live cells, cell surface proteoglycans, and glycans
Sponges, i.e., *Microciona prolifera*, *Halichondria panicea*, *Suberites fuscus*, and *Cliona celata* were collected by the Marine Biological Laboratory Marine Resources Dept. Live sponge cells were isolated as described previously (Misevic et al., 1987). Isolation of cell surface proteoglycans and pronase digestion of the core protein 200-kD glycans were performed as described previously (Misevic et al., 1987).

Analytical methods
For amino acid analyses, dry glycan samples were diluted in 1-ml of ultra pure water and the aliquots of 25 μl were lyophilized and hydrolyzed during 24 h. After hydrolysis, the black residues were suspended in 100 μl of 50 mM HCl containing 50 pmol/μl Sar and Nva each while ultrasonicated for 15 min. After a 15-min centrifugation, the transparent solutions were transferred into new reagent tubes and analyzed on a Hewlett-Packard AminoQuant II analyzer.

Aggregation assay
4.5×10^8 freshly sonified amine-modified beads (1-μm diam; Molecular Probes) were coupled with isolated glycans (1.5 mg/ml) by incubation in Ca^{2+}- and Mg^{2+}-free artificial seawater buffered with 20 mM Tris, pH 7.4, supplemented with 2 mM $CaCl_2$ (CSW), and 2 mg of 5,5′-dithiobis-(2-nitrobenzoic acid) (Molecular Probes) overnight at RT. Coupling efficiency was determined by measuring the glycan concentration (by staining with 1% Toluidine blue) on the beads after reversing the 5,5′-dithiobis-(2-nitrobenzoic acid) cross-linking with the disulfide-reducing agent DTT. The number of 200-kD glycan molecules bound per bead was calculated from the specific absorbance of stained glycans, which gave the number of moles (0.192×10^{-11}) multiplied by Avogadro's number (6.022×10^{23}), and was divided by the number of beads (4.5×10^8).

9×10^6 glycan-coated beads in 400 μl of CSW were allowed to aggregate with cells or other glycan-coated beads on a rotary shaker at 60 rpm for 4 h after the addition of 10 mM $CaCl_2$. Images of aggregates were acquired with a confocal laser-scanning microscope (Leica) equipped with an argon/krypton laser and a 10× objective (PL Fluotar, N.A. 0.3). Image processing was performed using Adobe Photoshop version 6.0. Quantifications were performed using UTHSCSA Image Tool version 2.00 Alpha.

Binding of cells and glycans to glycan-coated plates
Solutions of 200-kD glycans in CSW were placed in each well of a 96-well plastic plate (Falcon; 0.3 ml/well vol). After 2 h, each well was washed with CSW, 100 μl of glycans in 0.1 mg/ml CSW were added and incubated for 2 h at RT, after addition of 10 mM $CaCl_2$. Afterwards, nonbound glycans were washed off with CSW containing 10 mM $CaCl_2$. Bound glycans were stained with 1% Toluidine blue and absorbance was measured at 630 nm. The absorbance of glycans used as a coat was deducted from the total absorbance measured after the addition of glycans to coated wells to give the absorbance of bound glycans.

100 μl of live cells (5×10^3) in CSW were added to each glycan-coated well, supplemented with 200 μl of CSW containing 10 mM $CaCl_2$ and incubated for 2 h at RT. Afterwards, plates were immersed in CSW with 10 mM $CaCl_2$ in a large container, suspended upside down for 10 min with gentle shaking to allow nonadherent cells to sediment out of plates. Bound cells were lysed for 10 min in 2 M NaCl, 20 mM Tris-HCl, pH 7.5. 200 ng Hoechst stain in 20 mM Tris-HCl, pH 7.5, was added to cell lysates and the fluorescence was measured at $\lambda_{ex} = 360$ nm and $\lambda_{em} = 450$ nm.

AFM
Force measurements were performed with a commercial Nanoscope III AFM (Digital Instruments) equipped with a 162-μm scanner (J-scanner) and oxide-sharpened Si_3N_4 cantilevers with a thickness of 400 nm and a length of 100 μm. Cantilever spring constants k measured according to Chon et al. (2000) for a series of cantilevers from the same region of the wafer revealed on average k = 0.085 N/m and SD = 0.002 N/m. We observed a variation of <15% for k values from different cantilever batches. However, all measurements were done with cantilevers from the same batch.

AFM supports were built as described previously (Müller et al., 1999). The mica was cleaved using scotch tape, masked using a plastic ring mask with an inner diameter of 5 mm, and brought into the vacuum chamber of the gold sputter coater (Bal-Tec SCD 050). A vacuum of 10^{-2} mbar was generated and interspersed by rinsing the chamber with argon gas. At the pressure of 5×10^{-2} mbar a 20-nm gold layer was deposited on the mica surface and the tip controlled by a quartz thickness and deposition rate monitor (Bal-Tec QSG 050). Gold coated Si_3N_4 tips and micas allowed covalent chemisorptions of the naturally sulfated carbohydrates. Both the support and the tip were overlaid with CSW containing 10 mM $CaCl_2$ and the gold–gold interaction was measured. Afterwards, the support and the tip were incubated with isolated glycans (1 mg/ml) for 15 min at RT. Nonbound glycans were washed off with CSW, and glycan–glycan force measurements were performed in CSW containing 10 mM $CaCl_2$. For each measurement, a new tip was coated with 200-kD glycan and a new Au substrate was prepared. The AFM stylus approached and retracted from the surface ~100 times with a speed of 200 nm/s. The tip was moved laterally by 50 nm after recording five force-distance curves.

Surface clustering of 200-kD glycans was determined by fluorescence imaging. Glycans were labeled through their amino groups of the amino acid portion with 5(6)-carboxyfluorescein-*N*-hydroxysuccinimidester (Boehringer). Labeled glycans were separated from free labeling substance via a P-6 sizing column (Amersham Biosciences) in 100 mM pyridine-acetate buffer, pH 5.0.

References

Alonso, J.L., and W.H. Goldmann. 2003. Feeling the forces: atomic force microscopy in cell biology. *Life Sci.* 72:2553–2560.

Burger, M.M. 1979. The role of intercellular signals: navigation, encounter, outcome. *In* Life Sciences Research Report 14. J.G. Nicholls, editor. Verlag Chemie GmbH, Weinheim, Germany. 119–134.

Carrion-Vazquez, M., A.F. Oberhauser, T.E. Fisher, P.E. Marszalek, H. Li, and J.M. Fernandez. 2000. Mechanical design of proteins studied by single-molecule force spectroscopy and protein engineering. *Prog. Biophys. Mol. Biol.* 74:63–91.

Chon, J.W.M., P. Mulvaney, and J.E. Sader. 2000. Experimental validation of theoretical models for the frequency response of atomic force microscope cantilever beams immersed in fluids. *J. Appl. Physics.* 87:3978–3988.

Dammer, U., O. Popescu, P. Wagner, D. Anselmetti, H.J. Guntherodt, and G.N. Misevic. 1995. Binding strength between cell adhesion proteoglycans measured by atomic force microscopy. *Science.* 267:1173–1175.

de la Fuente, J.M., A.G. Barrientos, T.C. Rojas, J. Rojo, J. Canada, A. Fernandez, and S. Penades. 2001. Gold glyconanoparticles as water-soluble polyvalent models to study carbohydrate interactions. *Angew. Chem. Int. Ed. Engl.* 40:2257–2261.

Eggens, I., B. Fenderson, T. Toyokuni, B. Dean, M. Stroud, and S. Hakomori. 1989. Specific interaction between Lex and Lex determinants. A possible basis for cell recognition in preimplantation embryos and in embryonal carcinoma cells. *J. Biol. Chem.* 264:9476–9484.

Feizi, T. 2000. Progress in deciphering the information content of the "glycome"–a crescendo in the closing years of the millennium. *Glycoconj. J.* 17:553–565.

Feizi, T., and R.W. Loveless. 1996. Carbohydrate recognition by Mycoplasma pneumoniae and pathologic consequences. *Am. J. Respir. Crit. Care Med.* 154(4 Pt 2):S133–S136.

Fernandez-Busquets, X., and M.M. Burger. 2003. Circular proteoglycans from sponges: first members of the spongican family. *Cell. Mol. Life Sci.* 60:88–112.

Fritz, J., A.G. Katopodis, F. Kolbinger, and D. Anselmetti. 1998. Force-mediated kinetics of single P-selectin/ligand complexes observed by atomic force microscopy. *Proc. Natl. Acad. Sci. USA.* 95:12283–12288.

Galtsoff, P.S. 1925. Regeneration after dissociation: an experimental study on

sponges. *J. Exp. Zool.* 42:223–251.

Grandbois, M., M. Beyer, M. Rief, H. Clausen-Schaumann, and H.E. Gaub. 1999. How strong is a covalent bond? *Science.* 283:1727–1730.

Hanley, W., O. Mc, S. Carty, Y. Jadhav, D. Tseng, K. Wirtz, and K. Konstantopoulos. 2003. Single molecule characterization of P-selectin/ligand binding. *J. Biol. Chem.* 278:10556–10561.

Haseley, S.R., H.J. Vermeer, J.P. Kamerling, and J.F.G. Vliegenthart. 2001. Carbohydrate self-recognition mediates marine sponge cellular adhesion. *Proc. Natl. Acad. Sci. USA.* 98:9419–9424.

Hinterdorfer, P., W. Baumgartner, H.J. Gruber, K. Schilcher, and H. Schindler. 1996. Detection and localization of individual antibody-antigen recognition events by atomic force microscopy. *Proc. Natl. Acad. Sci. USA.* 93:3477–3481.

Humphreys, T. 1963. Chemical dissolution and *in vitro* reconstruction of sponge cell adhesions. I. Isolation and functional demonstration of the components involved. *Dev. Biol.* 53:27–47.

Hynes, R.O., and Q. Zhao. 2000. The evolution of cell adhesion. *J. Cell Biol.* 150:89–95.

Iwabuchi, K., S. Yamamura, A. Prinetti, K. Handa, and S. Hakomori. 1998. GM3-enriched microdomain involved in cell adhesion and signal transduction through carbohydrate-carbohydrate interaction in mouse melanoma B16 cells. *J. Biol. Chem.* 273:9130–9138.

Jarchow, J., J. Fritz, D. Anselmetti, A. Calabro, V.C. Hascall, D. Gerosa, M.M. Burger, and X. Fernandez-Busquets. 2000. Supramolecular structure of a new family of circular proteoglycans mediating cell adhesion in sponges. *J. Struct. Biol.* 132:95–105.

Jumblatt, J.E., V. Schlup, and M.M. Burger. 1980. Involvement of a carbohydrate group in the active site for surface guided reassociation of animal cells. *Biochemistry.* 19:1038–1042.

Kjellen, L., and U. Lindahl. 1991. Proteoglycans: structures and interactions. *Annu. Rev. Biochem.* 60:443–475.

Kojima, N., and S. Hakomori. 1989. Specific interaction between gangliotriaosylceramide (Gg3) and sialosyllactosylceramide (GM3) as a basis for specific cellular recognition between lymphoma and melanoma cells. *J. Biol. Chem.* 264:20159–20162.

Misevic, G.N., and M.M. Burger. 1993. Carbohydrate-carbohydrate interactions of a novel acidic glycan can mediate sponge cell adhesion. *J. Biol. Chem.* 268:4922–4929.

Misevic, G.N., J. Finne, and M.M. Burger. 1987. Involvement of carbohydrates as multiple low affinity interaction sites in the self-association of the aggregation factor from the marine sponge Microciona prolifera. *J. Biol. Chem.* 262:5870–5877.

Müller, D.J., W. Baumeister, and A. Engel. 1999. Controlled unzipping of a bacterial surface layer with atomic force microscopy. *Proc. Natl. Acad. Sci. USA.* 96:13170–13174.

Pickover, C.A. 2001. Wonders of numbers. Oxford University Press, Oxford, UK. 416 pp.

Popescu, O., I. Checiu, P. Gherghel, Z. Simon, and G.N. Misevic. 2003. Quantitative and qualitative approach of glycan-glycan interactions in marine sponges. *Biochimie.* 85:181–188.

Rief, M., F. Oesterhelt, B. Heymann, and H.E. Gaub. 1997. Single molecule force spectroscopy on polysaccharides by atomic force microscopy. *Science.* 275:1295–1298.

Robinson, S.D., P.S. Frenette, H. Rayburn, M. Cummiskey, M. Ullman-Cullere, D.D. Wagner, and R.O. Hynes. 1999. Multiple, targeted deficiencies in selectins reveal a predominant role for P-selectin in leukocyte recruitment. *Proc. Natl. Acad. Sci. USA.* 96:11452–11457.

Saleh, O.A., and L.L. Sohn. 2003. Direct detection of antibody-antigen binding using an on-chip artificial pore. *Proc. Natl. Acad. Sci. USA.* 100:820–824.

Song, Y., D.A. Withers, and S. Hakomori. 1998. Globoside-dependent adhesion of human embryonal carcinoma cells, based on carbohydrate-carbohydrate interaction, initiates signal transduction and induces enhanced activity of transcription factors AP1 and CREB. *J. Biol. Chem.* 273:2517–2525.

Spillmann, D., and M.M. Burger. 1996. Carbohydrate-carbohydrate interactions in adhesion. *J. Cell. Biochem.* 61:562–568.

Spillmann, D., K. Hard, J.E. Thomas-Oates, J.F. Vliegenthart, G. Misevic, M.M. Burger, and J. Finne. 1993. Characterization of a novel pyruvylated carbohydrate unit implicated in the cell aggregation of the marine sponge Microciona prolifera. *J. Biol. Chem.* 268:13378–13387.

Spillmann, D., J.E. Thomas-Oates, J.A. van Kuik, J.F. Vliegenthart, G. Misevic, M.M. Burger, and J. Finne. 1995. Characterization of a novel sulfated carbohydrate unit implicated in the carbohydrate-carbohydrate-mediated cell aggregation of the marine sponge Microciona prolifera. *J. Biol. Chem.* 270:5089–5097.

Stipp, C.S., and M.E. Hemler. 2000. Transmembrane-4-superfamily proteins CD151 and CD81 associate with alpha 3 beta 1 integrin, and selectively contribute to alpha 3 beta 1-dependent neurite outgrowth. *J. Cell Sci.* 113:1871–1882.

Tromas, C., J. Rojo, J.M. De La Fuente, A.G. Barrientos, R. Garcia, and S. Penades. 2001. Adhesion forces between Lewis[x] determinant antigens as measured by atomic force microscopy. *Angew. Chem. Int. Ed. Engl.* 40:3052–3055.

Truant, S., E. Bruyneel, V. Gouyer, O. de Wever, F.R. Pruvot, M. Mareel, and G. Huet. 2003. Requirement of both mucins and proteoglycans in cell-cell dissociation and invasiveness of colon carcinoma HT-29 cells. *Int. J. Cancer.* 104:683–694.

Turner, S.R., and M.M. Burger. 1973. Involvement of a carbohydrate group in the active site for surface guided reassociation of animal cells. *Nature.* 244:509–510.

Varki, A. 1994. Selectin ligands. *Proc. Natl. Acad. Sci. USA.* 91:7390–7397.

Wilson, H.V. 1907. On some phenomena of coalescence and regeneration in sponges. *J. Exp. Zool.* 5:245–258.